Surface enhanced electron correlation on the trivial quasi-two-dimensional bulk insulator 1*T*-TaS_2

Jiwon Jung,[1,2] Jae Whan Park,[1] Jaeyoung Kim,[1,*] and Han Woong Yeom[1,2,†]

[1]*Center for Artificial Low Dimensional Electronic Systems, Institute for Basic Science (IBS), Pohang 37673, Republic of Korea*

[2]*Department of Physics, Pohang University of Science and Technology (POSTECH), Pohang 37673, Republic of Korea*

(Received 28 January 2022; revised 13 August 2022; accepted 28 September 2022; published 10 October 2022)

While the prototypical quasi-two-dimensional charge density wave system of 1*T*-TaS_2 has been known as a Mott insulator with a possibility of quantum spin liquid, recent band-structure calculations and spectroscopic works in parallel suggested a metallic system or a spin-singlet insulator due to the interlayer coupling. Here, we carefully reinvestigate the out-of-plane electron dispersion, which reflects the interlayer electronic coupling, with angle-resolved photoelectron spectroscopy. We identify two distinct branches for the topmost valence band, which can be unambiguously related to the surface and the bulk layers with different band gaps. Density functional theory calculations clearly indicate a trivial band insulator due to the interlayer coupling for the bulk but the surface band gap affected substantially by the electron correlation. The surface-bulk electronic dichotomy consistently incorporates most of the theoretical and spectroscopic results reported so far and has wide implications for van der Waals materials with nontrivial interlayer interactions.

DOI: 10.1103/PhysRevB.106.155406

I. INTRODUCTION

Charge density waves (CDWs) in layered transition metal dichalcogenides host intriguing physics issues such as metal-insulator transition [1,2], commensurate-incommensurate transitions [3,4], hidden orders [5], and emerging superconductivity [6–8]. These issues are closely related to functionalities such as ultrafast switching devices [9] and memristors [10–13]. While monolayer systems in the two-dimensional (2D) limit of these materials are attracting updated interest [14,15], the interlayer coupling in their bulk forms is often substantial but not clearly addressed with a number of open questions [16–18]. Pinning down the effect of the interlayer coupling is important for understanding not only bulk properties but also layer-dependent properties in thinning the materials to reach their 2D limit.

1*T*-TaS_2 is a paradigmatic example with emerging many-body physics from quasi-2D CDW and intriguing interlayer coupling. It features an unusually rich phase diagram of various CDW states [5] and emerging superconductivity [6–8]. Upon cooling down from a metallic phase, 1*T*-TaS_2 exhibits an incommensurate CDW phase below 550 K and a nearly commensurate CDW with a domain-wall network below 350 K and a fully commensurate CDW (CCDW) below 180 K. The basic building block of nearly and fully commensurate CDW structures is the so-called David- star (DS) cluster, which is composed of 13 Ta atoms, each with a single 5*d* electron [Fig. 1(a)]. In the CCDW phase, the DS clusters form a $(\sqrt{13} \times \sqrt{13})R13.9^\circ$ superstructure. Due to the odd number of electrons in this unit cell, the CCDW phase has a half-filled band with its electrons localized on the central Ta atom of each DS cluster and with a very small bandwidth reflecting the large unit cell. The sizable on-site Coulomb repulsion of the 5*d* electron and the small bandwidth naturally lead to the Mott insulator model for the insulating phase below 180 K [19–22]. This model has been applied to explain various properties including domain-wall electronic structures [23–25] and hidden orders [26–31], and fueled the quantum spin liquid scenario for the absence of a magnetic order [32,33].

Since this model is based basically on 2D monolayer physics, it can be substantially affected by the interlayer coupling. Recent experimental and density-functional theory (DFT) studies favored the bilayer stacking order called the AC stacking [Fig. 1(a)], where two neighboring layers are stacked without a lateral translation (A) and each bilayer is stacked with a half-unit-cell translation (C) [34,35]. This stacking brings about strong interactions between half-filled d_{z^2} orbitals at the DS centers, which leads to the formation of a interbilayer spin singlet. The insulating property can then be explained by the trivial bonding-antibonding gap. However, there are important unsolved issues too. While the bulk stacking structure contains partial disorder [36,37], the disorder itself is not fully characterized and the detailed temperature dependence of the stacking order is not fully clear yet [38]. Moreover, the previous angle-resolved photoelectron spectroscopy (ARPES) experiments on the out-of-plane dispersion is not fully consistent with the calculations; the experiment reported a metallic band, which is consistent only with the other type of the stacking order (so-called L stacking), where all layers are translatively stacked [18,39]. More importantly, the trivial band insulator model is apparently not consistent with various spectroscopic signatures of strong electron correlation [23–27,40–47].

In this paper, we carefully reinvestigate the out-of-plane band structure of 1*T*-TaS_2 by ARPES and DFT calculations. We identify two predominent bands with distinct k_z dispersions, that is, dispersive and nondispersive bands both with clear band gaps. This rules out a metallic out-of-plane dis-

*jaeyoung@ibs.re.kr
†yeom@postech.ac.kr

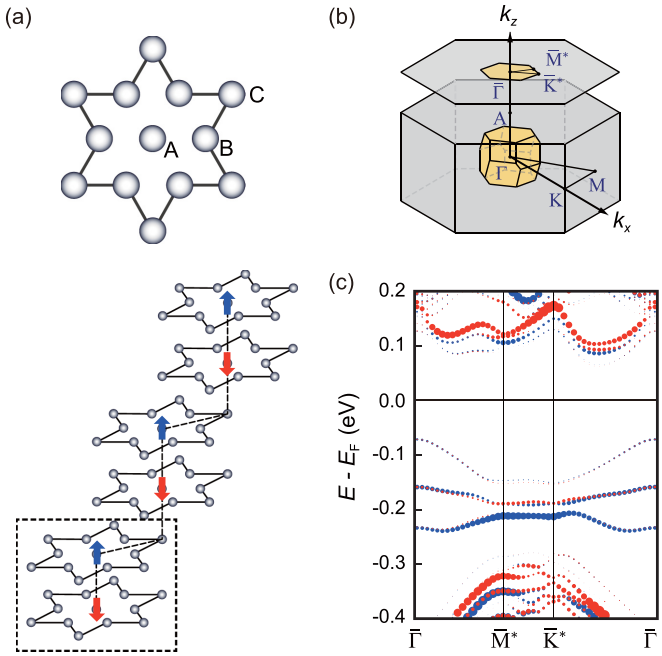

FIG. 1. Reconstructed atomic and electronic structure of 1*T*-TaS_2. (a) Reconstructed Ta structure of a CDW unit cell in 1*T*-TaS_2 and its popular stacking model. Dashed box denotes this $\times 2$ AC stacking order. Interbilayer spin (arrows) singlets are assumed. (b) Bulk and surface Brillouin zone of 1*T*-TaS_2. (c) Calculated in-plane band structure of a six layer slab model shown in (a). Blue and red circles denote the majority and minority spin, respectively. The size of dots in (c) is proportional to the electron weight at the top Ta layer. The three topmost bands are mainly localized on the first, second, and third layers, respectively, from the bottom.

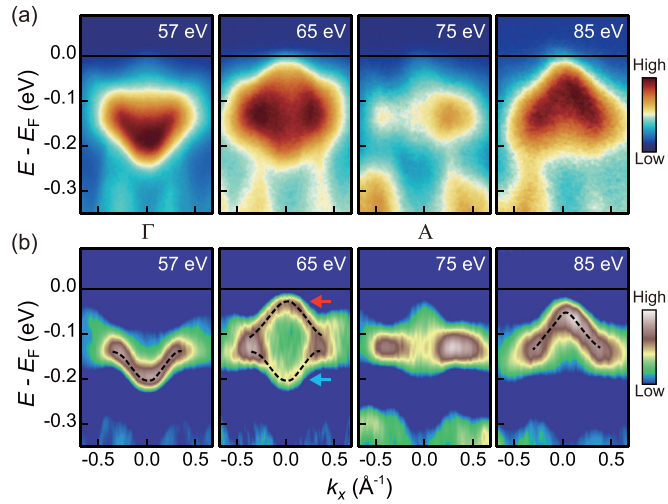

FIG. 2. Photon energy dependence of in-plane band structure. (a) ARPES intensity plots along the in-plane Γ-*K* direction of 1*T*-TaS_2 taken at varied photon energies of 57, 65, 75, and 85 eV taken at 10 K. (b) Second derivatives of the ARPES intensity maps for the same data sets in (a). The coexistence of two different bands near the Fermi level is indicated by dashed lines with red and blue arrows for the data at 65 eV.

persion and the translatively stacked (L) model [18,39]. The band-structure calculation identifies these two bands as a bulk and a surface band, respectively. The bulk band is consistent with the bilayer stacking with a trivial bonding-antibonding gap but the surface layer is inherited with a substantial contribution of the electron correlation in its band gap. The surface layer is, thus, close to a Mott-Peierls insulator. Note also that there can be another type of surface termination, the intrabilayer termination, which leads to a 2D-like Mott insulating behavior [48–50]. We thus conclude that the Mott physics of 1*T*-TaS_2 is restricted to the surface layers and possibly in the bulk with a stacking disorder [38]. This paper suggests that the major discrepancy between the experiments may largely be due to the difference of surface and bulk probes. The enhanced electron correlation on surface layers provides a general route to the emergence of a unique electronic phase in the layered materials.

II. METHODS

Commercial 1*T*-TaS_2 crystals (HQ graphene) were grown using the chemical vapor transport (CVT) method, whose quality was confirmed by the resistivity and x-ray measurements (see Fig. 1 in the Supplemental Material [51]). The single crystal 1*T*-TaS_2 was cleaved in ultrahigh vacuum for ARPES experiments using horizontally polarized light from the undulator Beamline 4A2 in the Pohang Light Source (Pohang, Korea). ARPES spectra were measured with the photon energy varied from 55 to 150 eV. The k_z resolution is limited by the inelastic mean-free path of photoelectrons, which is in total better than 0.2 Å^{-1} and the energy (angular) resolution were set to better than 10 meV (0.1 °). We performed DFT calculations using VIENNA AB INITIO SIMULATION PACKAGE [52] within the generalized gradient approximation [53] and the projector-augmented wave method [54]. We used a plane-wave basis set cutoff at 259 eV and the *k*-point sampling on a $8 \times 8 \times 8$ mesh for a $\sqrt{13} \times \sqrt{13} \times 2$ unit cell. All atoms were relaxed until the residual force components are within 0.03 eV Å^{-1} but the interlayer distance was fixed at the experimental value of 5.9 Å [55]. For the electronic correlation, we included an on-site Coulomb energy U of Ta 5*d* as 2.3 eV, which was widely used in the previous works [18]. The 1*T*-TaS_2 surface was simulated with a slab thickness of six layers and a vacuum spacing of about 15 Å [Fig. 1(a)]. The calculated bands in the superstructure were unfolded [56] for comparison with the experiments.

III. RESULTS AND DISCUSSION

The ARPES spectra obtained along the in-plane momemtum k_x [Γ-*K* direction in Fig. 1(b)] are shown in Fig. 2. The well-known topmost valence band is shown with a sinusoidal dispersion at $-0.1 \sim -0.2$ eV. The band gap at the Fermi level was attributed to a Mott gap [2] or a bonding-antibonding splitting due to the interlayer coupling [34,35]. The energy gap below this band at around -0.25 eV has been understood from the formation of the CDW superstructure [4]. The spectra recorded with the photon energy varied systematically exhibit a strong variation of the dispersion; an electronlike dispersion dominating for the photon energy of 57 eV around -0.2 eV of Γ but a holelike one for 85 eV at

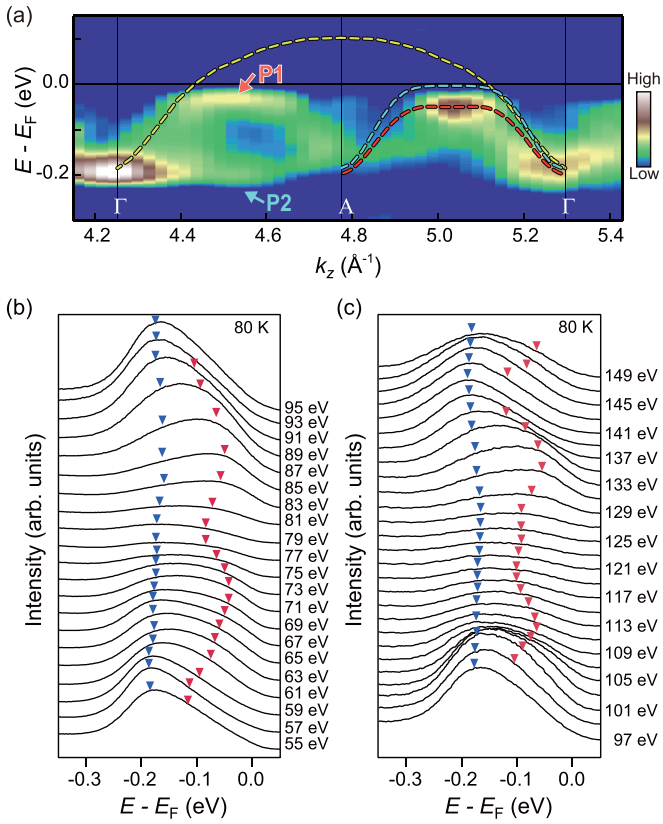

FIG. 3. Experimental and theoretical band structures along k_z direction. (a) Out-of-plane band dispersion of $1T$-TaS_2 along Γ-A as measured by second-derivative normal emission ARPES spectra taken at 80 K with the photon energy varied from 55 to 150 eV, which is overlaid with bulk bands calculated for the A stacking with DFT + U (yellow dashed line) [18], the AC stacking with DFT (the extra electron correlation U excluded, orange dashed line) [34], and the same AC stacking with DFT + U (red dashed line). We set the values of the inner potential $V_0 = 17$ eV and the work function $\Phi_0 = 4.5$ eV, which yield consistent Γ points with the previously reported ones [39,57]. (b), (c) The normal emission ARPES energy distribution curves (EDCs) taken at 80 K with denoted photon energies. At least two spectral features (the red and blue arrow heads, P1 and P2, respectively) are needed to explain the EDCs.

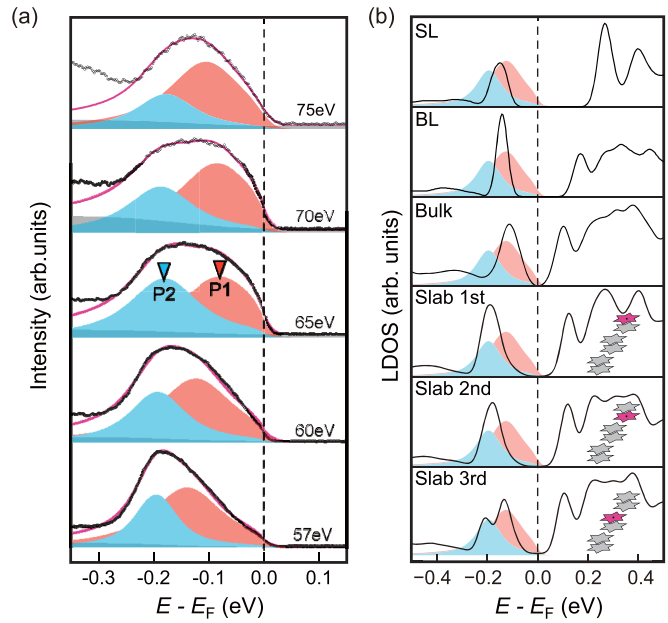

FIG. 4. Experimental and theoretical two spectral components. (a) ARPES energy distribution curves taken along normal emission (Γ) with different photon energies indicated. The curves are fit with standard Voight line shape of photoelectrons with backgrounds and a Fermi-Dirac distribution function. Two main components P1 and P2 are indicated with different colors. (b) Layer-resolved partial density of states calculated for the bulk or surface (or subsurface) layer (BL/SL) are compared with the fitted spectral components of the energy distribution curve at 57 eV (corresponding to the bulk Γ point). The surface (P2) and bulk (P1) contributions are clearly distinguished, although the slab calculation for the third layer still contains finite intermixing with the upper layers.

−0.04 eV in Fig. 2. This indicates a strong k_z dispersion of the band, especially at Γ. The electronlike dispersion at low photon energy is in good agreement with most of the previous ARPES studies of the CCDW phase [17,39,44,58,59] and the holelike dispersion at 85 eV was observed in the recent ARPES result [34]. The latter work indicated that the band touches the Fermi level with almost a zero gap and suggested the AC stacking order to explain this k_z dispersion [34]. Note also that another recent ARPES study of the k_z dispersion indicates a fully metallic dispersion [39]. However, these are not consistent with the present result of Fig. 2(a) and the more detailed presentation of the k_z dispersion in Fig. 3. The band gap persists with its minimum value of about 40 meV below the Fermi level. More importantly, we observe the coexistence of two separate bands, an electron-like and a hole-like band at the intermediate photon energies [see red and blue arrows in Figs. 2(b) and 3(a)]. In particular, note the dispersion-less feature extending from Γ at around −0.2 eV in the k_z dispersion [Figs. 3(a)]. This clearly indicate the existence of two components of non-dispersive and dispersive bands for the photon energy range scanned. This behavior cannot be explained by the mere broadening of the strong spectral peak at Γ due to its presence in almost a whole Brillouin zone. The existence of two separate bands, one with a strong k_z dispersion and the other without [Fig. 3(a)], can be corroborated by the strange shape of the ARPES EDC's shown in Fig. 4(a). These curves have to be fit with at least two spectral components (P1 and P2) (see also Fig. 2 in the Supplemental Material [51]), while the exact peak positions have uncertainty due to broad spectral widths. We note that a very early ARPES study performed at a much lower photon energy range reported two spectral features [61], which are consistent with the present observation. The discrepancies from the recent ARPES studies, the existence of the band gap and two split bands, provide important insights into the complicated physics of $1T$-TaS_2 as discussed below.

The out-of-plane band structure, especially for P1, in Fig. 3(a) show the folded band at the A point, which clearly indicates a doubled periodicity. This is consistent with the AC stacking order with a bilayer unitcell [34,35] but not compatible with the A or L stacking model of a primitive unitcell. Moreover, the observed dispersion clearly rules out

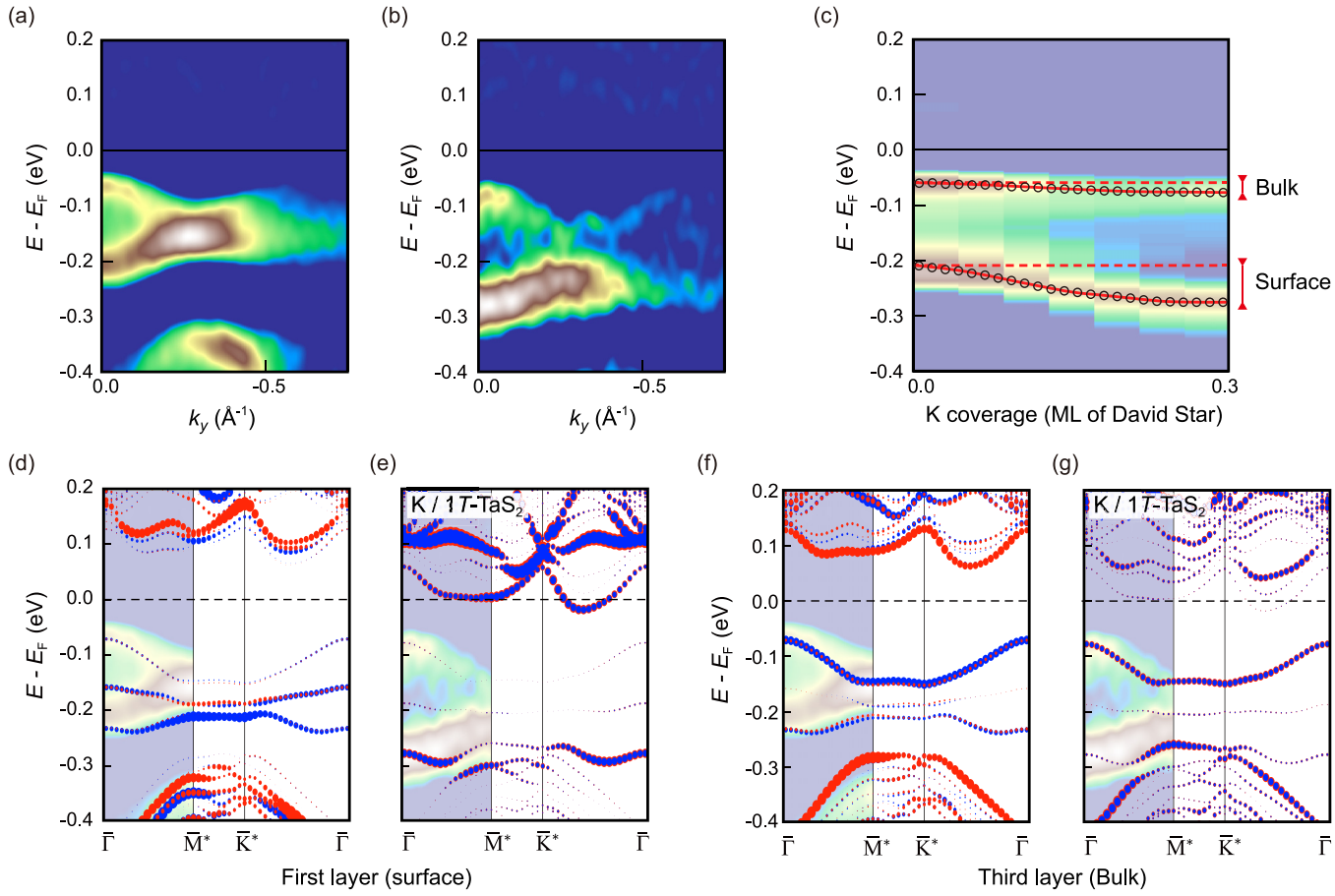

FIG. 5. Evolution of the in-plane band dispersions upon the surface adsorption of K atoms. (a), (b) Second derivative ARPES spectra along Γ-*M* direction for pristine and potassium (K) adsorbed 1T-TaS_2, respectively. The K coverage is about one in three DS unit cells. (c) Second derivative ARPES intensity at Γ point as a function of the K coverage. Comparison of the theoretical band structures for (d) [(f)] the pristine 1*T*-TaS_2 (a six layer slab as discussed above) for the first (third) layer with those of the K-adsorbed surface (e) [(g)]. The theoretical results are overlaid on the corresponding experimental data. This result excludes the interpretation of probed two-peak feature from the one band along k_z due to the photoelectron final states effect [60].

the A stacking, which predicts a metallic k_z dispersion. On the other hand, the k_z dispersion of the AC-stacked bulk is qualitatively consistent with the observation. It is also very obvious that any ordered stacking of layers cannot explain the extra dispersion-less band of P2.

In fact, a very recent ARPES study observed a distinct band with a little k_z dispersion appearing at a narrow temperature range around 225 K [38]. This state was attributed to a 2D-like Mott insulating phase induced by the full disordering in the interlayer stacking, which decouples bilayers in the AC stacking. Since our measurement is well within the temperature range of the CCDW phase where the bilayer AC stacking is largely preserved, this interpretation cannot be applied. As an alternative explanation, we note that the lack of k_z dispersion usually indicates a surface-localized electronic state and ARPES in this energy range is highly surface sensitive. To confirm this idea, the surface and bulk layers are modeled with a slab of three bilayers [Fig. 1(a)]. Figure 1(c) demonstrates the corresponding result of DFT + *U* calculations. The topmost valence band splits into three bands from each layer, which are degenerated doubly due to the inversion symmetry. The topmost band represents the most bulklike states in our model calculation as originating from the third layer. Its in-plane dispersion (holelike) is consistent with our ARPES observation of the dispersive band P1. On the other hand, the bottom and middle bands mainly comes from the first and second Ta layers, respectively, with some interlayer hybridization especially near the Γ point. While we cannot resolve these two bands, the experimental dispersion of the extra band P2 agrees with those of the surface layers. It is thus clear that the ARPES measurements reveal distinct bands originating from the bulk and surface layers with smaller and larger band gaps, respectively. In Fig. 4(b), the calculated LDOS of bulk and surface states are compared with the decomposition of the ARPES spectra (at 57 eV of Γ point). This comparison makes it more convincing that the ARPES spectra probes both the surface and bulk bands at higher and lower binding energies, respectively.

The surface origin of the extra band can be corroborated further. When the akali metal (K) is adsorbed on the surface, the two bands P1 and P2 exhibit distinctly different amount of energy shift to higher binding energies [Figs. 5(a)–5(c)]. These shifts can be well reproduced by DFT calculations adopting the K adsorption site at the center of each DS unit cell [Figs. 5(d)–5(g)], which was experimentally observed [49].

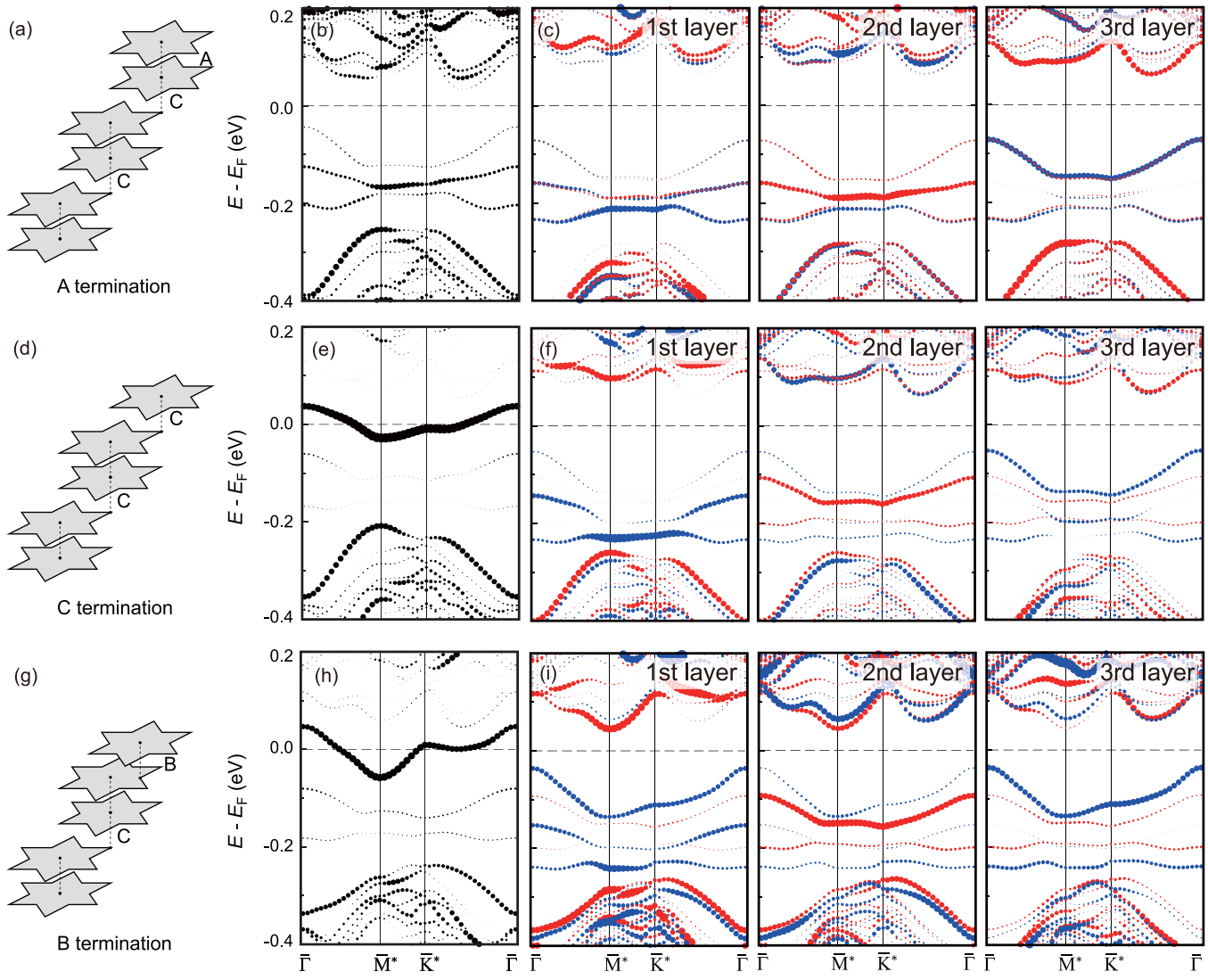

FIG. 6. Theoretical in-plane band structures of three different surface terminations. (a)–(c) A termination of six Ta layers, (d)–(f) C termination of five Ta layers, and (g)–(i) B termination (translated from the C termination) of five Ta layers. (b), (e), and (h) are without correlation effect and the circle size is proportional to the localized state at the first Ta layer. (c), (f), and (i) are for the denoted layers with electron correlation effect. Blue and red circles denote the majority and minority spin, whose size is proportional to the localized states on the denoted layer.

The origin of the bulk band gap is robustly clear as due to the interlayer bonding-antibonding splitting and is not affected substantially by the inclusion of the electron correlation (Figs. 6(b) and 6(c) and also Fig. 3 in the Supplemental Material [51]). This indicates unambiguously that the bulk is a trivial band insulator. However, it is different for the surface layer, as shown in Figs. 6(b) and 6(c). That is, roughly more than one-third of the whole band gap comes from the extra electron correlation in the topmost layer. It is clear that the surface layers (namely, the top two layers coupled) of the AC stacked $1T$-TaS_2 cannot be called as a simple band insulator. This situation is somewhat similar to a Mott-Peierls insulator [62] and the Peierls interaction corresponds to the interlayer dimerization in the present case. Theoretically speaking, it is now rather well-established that a correlated bilayer (dimer) system has a phase diagram with the Mott insulating and trivial insulator phases connected smoothly [62,63].

We have to consider the fact that recent scanning tunneling microscopy (STM) studies [48,49] reported different surface terminations on the surface with a different band-gap size. One termination is consistent with the present model and the other termination corresponds to the intrabilayer termination of the AC stacking. Our slab calculation for this termination indicates a metallic band without extra U but a Mott insulator with U in Fig. 6 (see also Fig. 4 in the Supplemental Material [51]). For this case, the surface layer band gap is solely decided by electron correlation and is thus consistent with a Mott insulating single layer. This is consistent with the case of a differently stacked interbilayer termination (so-called B termination) in Figs. 6(g)–6(i). These results can be straightforwardly understood if we consider the decoupled or undimerized d_z electrons in this surface layer. The surface-state band probed in the experiment thus can come from different terminations with different origins (and also

possibly different sizes) of the band gaps. This is consistent with a very recent theoretical work, which treated the electron correlation in a more sophisticated way [50]. This paper further interpreted the two components in ARPES as due to the contributions from surface areas with different terminations. Note, however, that our own experience with STM [49] and the very recent STM work [64] indicate that the intrabilayer termination appears only as minor cases, which seems to be due to the presence of domain walls within the surface layers. The different sensitivity on alkali adsorbates and the strong bulk dispersion supports the present interpretation with the bulk and surface components. On the other hand, The flat surface dispersion observed here cannot be explained by the partial, orientational, disorder of the bilayers, which was observed in the previous experiments [17,34,35]. Our DFT calculations (see Fig. 5 in the Supplemental Material [51]) show that such an orientational disorder between bilayers does not affect the bulk band dispersion substantially, which is mainly due to the bilayer bonding-antibonding splitting.

Finally, we comment on the possibility of out-of-plane magnetic orderings. While the ferromagnetically ordered bilayer structure shown in Fig. 1(a) is the most simple structure, a different superstructure is indicated with a periodicity doubled in the z direction (see Fig. 6 in the Supplemental material [51]). Such a larger superstructure can split the topmost band as shown, which induces an extra branch and the reduction in the bandwidth.

IV. CONCLUSIONS

This result seems closer to the observed band structure and may explain the broad spectral feature between P1 and P2 bands observed (see Fig. 2 in the Supplemental Material [51]). Considering the absence of a bulk magnetic ordering in the previous experiments [65], further investigation on the local out-of-plane magnetic ordering is requested. Such magnetic orderings and the existence of different surface terminations may contribute to the broad spectral widths observed in the experiment while our major finding of mainly two different bands from the bulk and surface layers remains unambiguous.

In conclusion, detailed photon-energy dependent ARPES measurements reveal two distinct branches in the topmost valence band of the CDW state of $1T$-TaS_2. With the aid of extensive DFT calculations, we identify the extra branch as originating from the surface layers. More importantly, the origin of the band gaps is different as the interlayer bonding-antibonding splitting in the bulk but a substantial electron correlation in the surface layers. The bulk-surface dichotomy explains the contradictory spectroscopic information from the probes with different surface sensitivity and introduce a novel route to highly correlated phases in layered materials.

ACKNOWLEDGMENT

This work was supported by the Institute for Basic Science (Grant No. IBS-R014-D1).

[1] J. A. Wilson and A. D. Yoffe, Adv. Phys. **18**, 193 (1969).
[2] P. Fazekas and E. Tosatti, Philos. Mag. B **39**, 229 (1979).
[3] J. A. Wilson, F. J. Di Salvo, and S. Mahajan, Adv. Phys. **24**, 117 (1975).
[4] K. Rossnagel, J. Phys.: Condens. Matter **23**, 213001 (2011).
[5] M. Yoshida, R. Suzuki, Y. Zhang, M. Nakano, and Y. Iwasa, Sci. Adv. **1**, e1500606 (2015).
[6] B. Sipos, A. F. Kusmartseva, A. Akrap, H. Berger, L. Forró, and E. Tutiš, Nat. Mater. **7**, 960 (2008).
[7] R. Ang, Y. Tanaka, E. Ieki, K. Nakayama, T. Sato, L. J. Li, W. J. Lu, Y. P. Sun, and T. Takahashi, Phys. Rev. Lett. **109**, 176403 (2012).
[8] P. Xu, J. O. Piatek, P.-H. Lin, B. Sipos, H. Berger, L. Forró, H. M. Rønnow, and M. Grioni, Phys. Rev. B **81**, 172503 (2010).
[9] C. J. Docherty, P. Parkinson, H. J. Joyce, M.-H. Chiu, C.-H. Chen, M.-Y. Lee, L.-J. Li, L. M. Herz, and M. B. Johnston, ACS Nano **8**, 11147 (2014).
[10] M. Wang, S. Cai, C. Pan, C. Wang, X. Lian, Y. Zhuo, K. Xu, T. Cao, X. Pan, B. Wang, S.-J. Liang, J. J. Yang, P. Wang, and F. Miao, Nat. Electron. **1**, 130 (2018).
[11] D. Li, B. Wu, X. Zhu, J. Wang, B. Ryu, W. D. Lu, W. Lu, and X. Liang, ACS Nano **12**, 9240 (2018).
[12] M. Kim, R. Ge, X. Wu, X. Lan, J. Tice, J. C. Lee, and D. Akinwande, Nat. Commun. **9**, 2524 (2018).
[13] R. Xu, H. Jang, M.-H. Lee, D. Amanov, Y. Cho, H. Kim, S. Park, H.-j. Shin, and D. Ham, Nano Lett. **19**, 2411 (2019).
[14] M. M. Ugeda, A. J. Bradley, Y. Zhang, S. Onishi, Y. Chen, W. Ruan, C. Ojeda-Aristizabal, H. Ryu, M. T. Edmonds, H.-Z. Tsai, A. Riss, S.-K. Mo, D. Lee, A. Zettl, Z. Hussain, Z.-X. Shen, and M. F. Crommie, Nat. Phys. **12**, 92 (2016).
[15] C. E. Sanders, M. Dendzik, A. S. Ngankeu, A. Eich, A. Bruix, M. Bianchi, J. A. Miwa, B. Hammer, A. A. Khajetoorians, and P. Hofmann, Phys. Rev. B **94**, 081404(R) (2016).
[16] Y. Ge and A. Y. Liu, Phys. Rev. B **82**, 155133 (2010).
[17] T. Ritschel, J. Trinckauf, K. Koepernik, B. Büchner, M. v. Zimmermann, H. Berger, Y. I. Joe, P. Abbamonte, and J. Geck, Nat. Phys. **11**, 328 (2015).
[18] P. Darancet, A. J. Millis, and C. A. Marianetti, Phys. Rev. B **90**, 045134 (2014).
[19] E. Dagotto, Rev. Mod. Phys. **66**, 763 (1994).
[20] M. Imada, A. Fujimori, and Y. Tokura, Rev. Mod. Phys. **70**, 1039 (1998).
[21] P. A. Lee, N. Nagaosa, and X.-G. Wen, Rev. Mod. Phys. **78**, 17 (2006).
[22] M. Nakano, K. Shibuya, D. Okuyama, T. Hatano, S. Ono, M. Kawasaki, Y. Iwasa, and Y. Tokura, Nature (London) **487**, 459 (2012).
[23] D. Cho, S. Cheon, K.-S. Kim, S.-H. Lee, Y.-H. Cho, S.-W. Cheong, and H. W. Yeom, Nat. Commun. **7**, 10453 (2016).
[24] D. Cho, G. Gye, J. Lee, S.-H. Lee, L. Wang, S.-W. Cheong, and H. W. Yeom, Nat. Commun. **8**, 392 (2017).
[25] L. Ma, C. Ye, Y. Yu, X. F. Lu, X. Niu, S. Kim, D. Feng, D. Tománek, Y.-W. Son, X. H. Chen, and Y. Zhang, Nat. Commun. **7**, 10956 (2016).
[26] L. Perfetti, P. A. Loukakos, M. Lisowski, U. Bovensiepen, H. Berger, S. Biermann, P. S. Cornaglia, A. Georges, and M. Wolf, Phys. Rev. Lett. **97**, 067402 (2006).
[27] L. Perfetti, P. A. Loukakos, M. Lisowski, U. Bovensiepen, M. Wolf, H. Berger, S. Biermann, and A. Georges, New J. Phys. **10**, 053019 (2008).

[28] S. Hellmann, M. Beye, C. Sohrt, T. Rohwer, F. Sorgenfrei, H. Redlin, M. Kalläne, M. Marczynski-Bühlow, F. Hennies, M. Bauer, A. Föhlisch, L. Kipp, W. Wurth, and K. Rossnagel, Phys. Rev. Lett. **105**, 187401 (2010).
[29] M. Eichberger, H. Schäfer, M. Krumova, M. Beyer, J. Demsar, H. Berger, G. Moriena, G. Sciaini, and R. J. Miller, Nature (London) **468**, 799 (2010).
[30] J. C. Petersen, S. Kaiser, N. Dean, A. Simoncig, H. Y. Liu, A. L. Cavalieri, C. Cacho, I. C. E. Turcu, E. Springate, F. Frassetto, L. Poletto, S. S. Dhesi, H. Berger, and A. Cavalleri, Phys. Rev. Lett. **107**, 177402 (2011).
[31] L. Stojchevska, I. Vaskivskyi, T. Mertelj, P. Kusar, D. Svetin, S. Brazovskii, and D. Mihailovic, Science **344**, 177 (2014).
[32] K. T. Law and P. A. Lee, Proc. Natl. Acad. Sci. **114**, 6996 (2017).
[33] M. Klanjšek, A. Zorko, R. Žitko, J. Mravlje, Z. Jagličić, P. Biswas, P. Prelovšek, D. Mihailovic, and D. Arčon, Nat. Phys. **13**, 1130 (2017).
[34] T. Ritschel, H. Berger, and J. Geck, Phys. Rev. B **98**, 195134 (2018).
[35] S.-H. Lee, J. S. Goh, and D. Cho, Phys. Rev. Lett. **122**, 106404 (2019).
[36] S. Tanda, T. Sambongi, T. Tani, and S. Tanaka, J. Phys. Soc. Jpn. **53**, 476 (1984).
[37] T. Ishiguro and H. Sato, Phys. Rev. B: Condens. Matter **44**, 2046 (1991).
[38] Y. D. Wang, W. L. Yao, Z. M. Xin, T. T. Han, Z. G. Wang, L. Chen, C. Cai, Y. Li, and Y. Zhang, Nat. Commun. **11**, 4215 (2020).
[39] A. S. Ngankeu, S. K. Mahatha, K. Guilloy, M. Bianchi, C. E. Sanders, K. Hanff, K. Rossnagel, J. A. Miwa, C. Breth Nielsen, M. Bremholm, and P. Hofmann, Phys. Rev. B **96**, 195147 (2017).
[40] J.-J. Kim, W. Yamaguchi, T. Hasegawa, and K. Kitazawa, Phys. Rev. Lett. **73**, 2103 (1994).
[41] J.-J. Kim, I. Ekvall, and H. Olin, Phys. Rev. B **54**, 2244 (1996).
[42] F. Zwick, H. Berger, I. Vobornik, G. Margaritondo, L. Forró, C. Beeli, M. Onellion, G. Panaccione, A. Taleb-Ibrahimi, and M. Grioni, Phys. Rev. Lett. **81**, 1058 (1998).
[43] F. Clerc, C. Battaglia, M. Bovet, L. Despont, C. Monney, H. Cercellier, M. G. Garnier, P. Aebi, H. Berger, and L. Forró, Phys. Rev. B **74**, 155114 (2006).
[44] S. Hellmann, T. Rohwer, M. Kalläne, K. Hanff, C. Sohrt, A. Stange, A. Carr, M. M. Murnane, H. C. Kapteyn, L. Kipp, M. Bauer, and K. Rossnagel, Nat. Commun. **3**, 1069 (2012).
[45] H. Sato, M. Arita, Y. Utsumi, Y. Mukaegawa, M. Sasaki, A. Ohnishi, M. Kitaura, H. Namatame, and M. Taniguchi, Phys. Rev. B **89**, 155137 (2014).
[46] D. Cho, Y.-H. Cho, S.-W. Cheong, K.-S. Kim, and H. W. Yeom, Phys. Rev. B **92**, 085132 (2015).
[47] I. Lutsyk, M. Rogala, P. Dabrowski, P. Krukowski, P. J. Kowalczyk, A. Busiakiewicz, D. A. Kowalczyk, E. Lacinska, J. Binder, N. Olszowska, M. Kopciuszynski, K. Szalowski, M. Gmitra, R. Stepniewski, M. Jalochowski, J. J. Kolodziej, A. Wysmolek, and Z. Klusek, Phys. Rev. B **98**, 195425 (2018).
[48] C. J. Butler, M. Yoshida, T. Hanaguri, and Y. Iwasa, Nat. Commun. **11**, 2477 (2020).
[49] J. Lee, K.-H. Jin, and H. W. Yeom, Phys. Rev. Lett. **126**, 196405 (2021).
[50] F. Petocchi, C. W. Nicholson, B. Salzmann, D. Pasquier, O. V. Yazyev, C. Monney, and P. Werner, Phys. Rev. Lett. **129**, 016402 (2022).
[51] See Supplemental Material at http://link.aps.org/supplemental/10.1103/PhysRevB.106.155406 for details of experimental data and theoretical results, which includes Refs. [6,17].
[52] G.-M. Zhang and A. C. Hewson, Phys. Rev. B **54**, 1169 (1996).
[53] J. P. Perdew, K. Burke, and M. Ernzerhof, Phys. Rev. Lett. **77**, 3865 (1996).
[54] P. E. Blöchl, Phys. Rev. B **50**, 17953 (1994).
[55] F. L. Givens and G. E. Fredericks, J. Phys. Chem. Solids **38**, 1363 (1977).
[56] V. Popescu and A. Zunger, Phys. Rev. B **85**, 085201 (2012).
[57] R. Manzke, O. Anderson, and M. Skibowski, J. Phys. C **21**, 2399 (1988).
[58] T. Pillo, J. Hayoz, H. Berger, M. Grioni, L. Schlapbach, and P. Aebi, Phys. Rev. Lett. **83**, 3494 (1999).
[59] K. Rossnagel, E. Rotenberg, H. Koh, N. V. Smith, and L. Kipp, Phys. Rev. Lett. **95**, 126403 (2005).
[60] E. E. Krasovskii, K. Rossnagel, A. Fedorov, W. Schattke, and L. Kipp, Phys. Rev. Lett. **98**, 217604 (2007).
[61] T. Pillo, J. Hayoz, D. Naumović, H. Berger, L. Perfetti, L. Gavioli, A. Taleb-Ibrahimi, L. Schlapbach, and P. Aebi, Phys. Rev. B **64**, 245105 (2001).
[62] O. Nájera, M. Civelli, V. Dobrosavljević, and M. J. Rozenberg, Phys. Rev. B **97**, 045108 (2018).
[63] M. Golor, T. Reckling, L. Classen, M. M. Scherer, and S. Wessel, Phys. Rev. B **90**, 195131 (2014).
[64] Z. Wu, K. Bu, W. Zhang, Y. Fei, Y. Zheng, J. Gao, X. Luo, Z. Liu, Y.-P. Sun, and Y. Yin, Phys. Rev. B **105**, 035109 (2022).
[65] F. J. DiSalvo and J. V. Waszczak, Phys. Rev. B **22**, 4241(1980).